IEEE Access
Multidisciplinary ⋮ Rapid Review ⋮ Open Access Journal

Received 21 April 2023, accepted 3 May 2023, date of publication 12 May 2023, date of current version 23 May 2023.

Digital Object Identifier 10.1109/ACCESS.2023.3275848

RESEARCH ARTICLE

Distributed Consensus Control Supported by High Reporting Rate Meters in Inverter-Based Cyber-Physical Microgrids

IGOR SOWA[1] AND ANTONELLO MONTI[1,2], (Senior Member, IEEE)
[1]Institute for Automation of Complex Power Systems, RWTH Aachen University, 52064 Aachen, Germany
[2]Fraunhofer FIT, 52064 Aachen, Germany

Corresponding author: Igor Sowa (isowa@eonerc.rwth-aachen.de)

This work was supported in part by the German Federal Ministry for Education and Research in the Context of Project Kopernikus Ensure Phase 2 under Grant 03SFK1C0-2.

ABSTRACT This paper presents formulation and analysis of a distributed consensus-based controller for power electronics based microgrids (MG) with grid forming (GFM) and grid feeding (GFD) inverters. The control is supported by measurements from high reporting rate meters that improve the dynamics of consensus control and enables participation of buses with no dispatchable units. The study is performed on a developed cyber-physical (CP) model in DQ domain that allows for the analysis of arbitrary MGs. The control is established on fundamental principles of consensus and provides power sharing and voltage regulation, maintains power reserve in MG, and assumes distinct roles for different types of inverters. The analysis of the control scheme includes aspects of coupling between cyber and physical layers and stability under multi-layer communication structure. The study addresses disadvantages of classical hierarchical control and enhances analysis of distributed controllers through the proposed CP model.

INDEX TERMS Microgrid, consensus, cyber-physical model, power sharing, grid forming inverter, grid feeding inverter, voltage control.

I. INTRODUCTION

Microgrids is a fast-growing topic that can resolve multiple challenges of the future power system. They can be superior comparing to classical power system structures considering efficiency, reliability, and flexibility as well as expandability [1]. The dominant control scheme for AC microgrids is based on assumptions from classical hierarchical power systems control [2], in which droop, secondary and tertiary control layers are responsible for frequency, voltage, power balance control in the network, also for power electronics based microgrids [3]. When it comes to communication in these three control layers, the droop control is usually a local control that does not require communication, while secondary and tertiary levels require at least low-bandwidth communication to a central entity that manages the control process [4].

In such architectures, voltage source inverters (VSI) usually operate in a similar way to classical synchronous generators (SG). While there are various control schemes proposed for droop-type control of VSI, the simplest and most common one controls active power with frequency deviation and reactive power with voltage deviation. The control mimics SG for frequency and voltage regulation, reducing frequency when active power increases and reducing the output voltage magnitude when the reactive power increases. Such droop mechanisms suffer, however, from coupling of control variables in case of resistive-inductive lines. Also, they lead to non-nominal steady state, while the transient performance can induce instability [5], [6], [7]. These drawbacks have been addressed through different improved droop strategies, e.g., in the power-synchronization control for VSIs, where some control techniques introduce synthetic inertia through filters [8] or additional power control loops [9], [10] that can limit frequency deviations [11], especially necessary in presence of other inertial elements in the network, such as SGs.

The associate editor coordinating the review of this manuscript and approving it for publication was Nagesh Prabhu.

Besides the primary level of control based on droop, in secondary control of classical hierarchical scheme, a single central entity processes all measurements, information, and control setpoints. In case of alternative design through distributed controllers, a single central entity is not necessary because processing of information is delegated to agents operating autonomously to realize global objectives [12]. In a microgrid, such agents can control distributed energy resources (DER) and their power inverters. Distributed control is often characterized by higher robustness, scalability, and plug-and-play capabilities [13], but also higher level of reliability and security and more compatibility with modern communication [14] or distributed applications [15].

As one of the distributed control methods, consensus-based control is often used in research for microgrid control schemes. Its principles are used in applications to achieve better power sharing, optimal dispatch [16], frequency and voltage restoration [17], but also for harmonics sharing and power quality improvements [18], [19]. The most popular types of consensus control are linear consensus schemes of first [20] or second orders [21], [22].

Due to its inherent need for communication, consensus is rarely used as primary controller, rather at secondary or tertiary control level. There are several recent studies on microgrid control schemes that rely on distributed control methods like consensus. These studies sometimes consider the consensus at primary control level, substituting classical droop, or more often as a secondary controller that is a part of more complex hierarchical scheme.

In [23] and [24], the authors exhaustively describe the consensus-based control that regulates active and reactive power in MG as a primary controller. Their results show that in case of reference variation at the nodes, the distributed architecture can realize accurate power sharing according to a ratio of rated power. The control is performed only among the nodes with unconstrained dispatchable resources, and it converges to unregulated average voltage level. The authors analyze only inductive networks limited to 4 sources and radial topology. In [22], control similar to droop is implemented in a multiagent-consensus architecture for frequency and voltage regulation and for only predefined, proportional power sharing. In their work, the authors do not analyze impact of delays or different communication topologies, or the control convergence issues related to physical network. In [25], a distributed control for MG is designed, but only for active power and frequency dynamics. They study associated stability in the partitioned system, identifying critical communication and physical links, but the delays of the cyber layer are not addressed. In [26], the authors design a distributed control without droop, but with robust distributed controller, which is used for active and reactive power sharing between subsystems with multiple DGs. Robustness is achieved through modelling and addressing uncertainties, but the impact from communication, cyber layer, control convergence is not addressed. In [27] and [28], optimal power dispatch controllers in the primary operation are designed. In [27], the power sharing is assumed proportional to the fixed ratings according to the centrally optimal objectives and the network consists of only 4 DG units connected to a feeder that creates radial microgrid under only limited communication scenarios. In [28], the optimal power sharing is achieved in the distributed way using a quasi-Newton distributed control method, but the operation is analyzed only under very low delays and simulations with only six generating or consuming units are performed, only under single, fixed delay. In [29], the authors propose a partially distributed control scheme that with a predictive voltage controller, where they focus on impact from data-loss and its mitigation in the proposed voltage hierarchical controller, but only small communication networks with single delays are considered, while the use cases are performed almost exclusively on radial microgrid. In [30], the consensus-based distributed controller for multi-functional grid-tied inverters focuses on quality improvements but considered physical and communication networks are limited to several nodes and thus, the impact from cyber layer dynamics is not investigated in detail. An interesting stochastic distributed control scheme is developed in [31] for voltage regulation in multi-inverter networks subject to communication delays, however only for small radial networks with simple communication network. In [32], a distributed secondary adaptive resilient control is designed to counter the effects of faults or attacks. Again, although the physical network used is a larger 33-bus system, only simple, single layer communication networks are considered. In [33], the authors propose the event-driven multi-layer consensus control scheme for DC microgrid clusters, with complex hierarchical communication scheme. The communication structure has fixed rules due to defined primary, secondary, and tertiary levels, therefore it is not arbitrary in terms of the communication structure. The authors do not consider impact from communication delays in the proposed scheme.

In the described literature [23], [24], [25], [26], [27], [28], [29], [30], [31], [32], [33], the researchers present different distributed MG controllers, which are inherently communication-based control schemes, often partially or fully based on consensus principles, operating jointly with droop, and sometimes in a droop-free schemes. Some studies address different scenarios of communication design, but usually with only single, fixed delays, and only for small communication networks, which are decoupled in the analysis from physical features of the grids. This excludes from analysis the situations when coupling of physical- and cyber-layers is critical for convergence, dynamics, and stability, especially under communication delays. In the studied communication-based controllers' use cases, usually only small electrical systems are considered, often only with radial or symmetrical design of electrical topology without larger and more complex, or arbitrary structures. The AC inverters assumed for the control are usually of the same type and follow the same strategy, i.e., divide to different types of inverters (such

as grid forming, grid feeding, grid following or supporting inverters) is not considered what might limit the practicality of the solutions in realistic networks. Only control at the buses where dispatchable units is considered, while buses without such devices are neglected, what might lead to violated voltage levels of buses that are not properly monitored.

Considering the identified research gaps in the existing literature, this paper proposes and analyzes distributed consensus control scheme for islanded MGs that considers dynamics of both cyber and physical layers for arbitrary electrical and communication topologies with different features. The proposed scheme includes explicit strategies for grid forming and grid feeding inverters and it is supported by high reporting rate meters, which provide additional measurements that can involve buses with no dispatchable resources in the system control. The control scheme effectively realizes primary and secondary control objectives for islanded microgrids in a single control layer. It is formulated and studied through the proposed CP model that considers arbitrary topology in physical- and cyber-layers, dynamics of both layers and coupling between them. The formulated CP model merges equations in the DQ domain and is used for analysis of dynamics in the consensus control for active and reactive power sharing and voltage regulation. Power electronics based microgrids including power inverters with limited (constrained) output power are considered.

The developed control scheme for grid forming and feeding inverters assumes maximizing power reserve of GFM inverters in order to increase MG resilience to large disturbances and it is able to actively control bus voltages through different inverters. As the results show, support of high reporting rate meters improves transient response of consensus control improves voltage profile of buses without dispatchable units. Effects of different conditions in physical- and cyber-layers, such as line impedances, communication delays and topologies, placement of meters are evaluated considering objectives of the framework. It is assumed that inverters and high reporting rate meters communicate with each other using modern communication that allows reduction of communication delay between devices geographically close to each other. The analysis is performed on larger networks in order to investigate scenarios of modern communication networks with multiple delays and different topology designs.

The contributions of this paper can be summarized as follows: (i) formulation and analysis is presented of distributed consensus control for inverter-based islanded microgrids supported by high reporting rate meters involving in control the buses with no dispatchable inverter units. (ii) Cyber-physical model for arbitrary networks is developed and the control convergence, dynamics and stability of the distributed consensus primary control is assessed considering its dependence from cyber and physical layers and coupling between them. (iii) Impact of different designs of cyber-layer's communication network is evaluated with respect to inverters' output current limits and global stability under multiple communication delays.

II. OBJECTIVES OF DISTRIBUTED CONSENSUS SUPPORTED BY HIGH REPORTING RATE METERS

It is assumed that the control objectives of distributed consensus control supported by measurements for islanded microgrids should correspond to classical hierarchical control with primary and secondary controllers, that is, it should provide control for frequency, voltage, and power sharing including restoring to nominal values. It is assumed that MG includes grid forming (GFM) and grid feeding (GFD) inverters [3], i.e., inverters that can form the AC voltage from frequency and voltage references and inverters that are able to infeed required amount of active and reactive power synchronizing to the measured voltage, respectively. The control is supported by measurements of active, reactive power and voltage magnitude from buses where high reporting rate meters are placed. In the following subsections, the objectives and assumptions of the proposed control scheme are generally described, while the details and equations are included Sections III-A and III-C.

A. POWER SHARING AND FREQUENCY CONTROL

In a normal mode of operation, it is assumed that the microgrid should maintain its power reserve available in order to cover power unbalance in case of a disturbance. Power reserve is maintained by GFM inverters, which as voltage source inverters (VSI) are inherently able to respond to the power imbalances in the network according to the voltage measured at their terminals. In order to maintain the power reserve of GFM inverters, their power response to a disturbance is distributed to GFD inverters, effectively realizing power sharing for MG. The information about power sharing is distributed by means of communication network and distributed consensus protocol instead of classical droop equations.

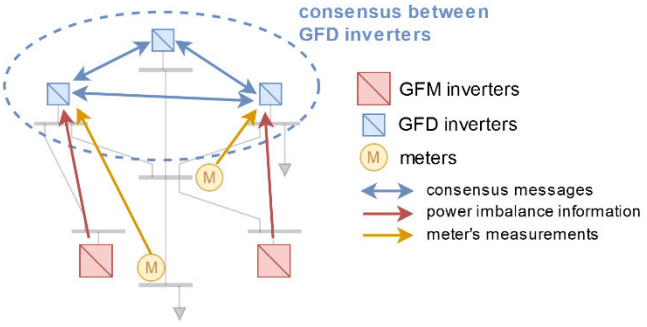

FIGURE 1. Exchange of information between GFM, GFD inverters and high-reporting rate meters in a simple MG.

In the Figure 1, one can see the simplest exemplary design of information distribution for power sharing, where the GFM inverters communicate messages about power imbalance to at least one GFD inverter, while GFD inverters execute the consensus control communicating with each other and receiving additional measurements from high reporting rate meters.

Details about the flow of information is presented in Section III.

The droop equations are only considered for GFM inverters for the purpose of synchronization. Since GFM inverters are critical for stability in the microgrid, it is important to distribute the imbalance to the GFD inverters as soon as possible, at the same time restoring the reserve power of GFM inverters in case of subsequent disturbances. This becomes even more important in small microgrids with only power electronics interfaced intermittent RES, where in case of large disturbance and resulting significant power imbalance, the GFM inverters can be subject to high current infeed what can be dangerous due to hardware limitations.

Each GFM inverter can keep the frequency reference at the nominal value that is only slightly internally modified for the purpose of synchronization. Excluding transient moments after disturbances, GFM inverters are able to maintain their frequency at its reference levels [24]. Therefore, no classical secondary control is necessary for restoring the frequency to the nominal levels. With no $P-f$ and $Q-V$ droop equations for power sharing, the coupling of active and reactive power does not appear, as the references are communicated directly by cyber links. Inverters transfer the information necessary for power sharing, following the distributed consensus control principles, instead of transferring this information through droop equations, which are subject to network dynamics and can become significantly distorted depending on the physical layer of the network.

On the other hand, the dynamics and stability are strongly related to the cyber layer of the system, i.e., communication, which is an inherent component when operating with distributed consensus. The delay in communicating information about power sharing is mostly related to cyber layer, namely to the communication latency, but also to the delay in propagation of consensus references that depends on communication topology. In classical hierarchical power sharing strategies with droop control, the total delay between the moment of a disturbance and an instant when the control setpoints are implemented includes network dynamics delays for $P-f$ and $Q-V$ curves, delays in internal control of GFM and GFD inverters including the PLL loop dynamics of GFD inverters. In the assumed distributed consensus control, power measurements from high reporting rate meters support the operation further reducing the delay between the moment of a disturbance and moment of interception of the power imbalance by GFD inverters. It is especially beneficial in case of reduced communication latency, e.g., when the measurement devices are in the vicinity of GFD inverters. Supporting measurements that can reflect the disturbance in the network are directly applied to internal control of GFD inverters, those who have access to the measurements. In this way, power imbalance interception by GFD inverters is accelerated, and convergence of the distributed consensus protocol to all other inverters is enhanced.

Strategies of power sharing based on classical hierarchical control like droop can be nonetheless a part of the proposed distributed consensus control supported by measurements, especially useful as a backup in case of lack of communication. In a framework of classical hierarchical control, presented strategy can be also considered as a distributed secondary control. Since the response dynamics can be comparable and even faster to the primary droop control-based power sharing, in this paper, it is considered that the consensus control supported by measurements operates without other control layers. If such strategy operates simultaneously with power sharing based on droop, interactions of dynamics should be investigated.

B. VOLTAGE CONTROL

In a normal mode of operation, the consensus control maintains power reserve of GFM inverters in order to cover power imbalance in case of a disturbance. When the voltage levels of the buses in the network are not violated, GFM inverters realize only the strategy of adjustment of their local voltages that leads to reduction of their reactive power infeed and thus maximization of available power reserve. After a disturbance, such as connection of new elements, a new steady state can appear including new bus voltage levels, especially for the buses closer to the disturbance. When the voltage levels are violated, voltage control is executed through the reactive power flow based on the consensus between the GFD inverters. The GFM inverters are also able to participate in the consensus voltage control, as they have direct control over their voltage references. Thus, they are able to shift the voltage of entire microgrid, still maintaining the objective of maximizing its power reserve. Networks with their R/X ratio close to 1 are studied in this work. Due to flexibility of the power electronics when generating reactive power almost independently from their DC side power availability, voltages are assumed to be controlled dominantly through the reactive power, although the coupling to active power exists and voltage control is also possible by means of active power.

In the presence of high reporting rate meters, which measure voltage magnitudes in different buses of the network, it is possible to include buses without dispatchable inverters into the consensus control (non-dispatchable buses). Such buses are not able to regulate their active and reactive power generation or consumption; however, the inverters at other buses are able to influence bus voltages in their proximity through active and reactive power regulation. Therefore, voltage control of non-dispatchable buses is possible indirectly through physical coupling. Consensus control with non-dispatchable buses is much more dependent on the physical dynamics of the network because bus voltages at the non-dispatchable buses can have multiple line connections, thus interdependencies with other buses, what might be more challenging for accurate control.

C. OTHER DISTRIBUTED STRATEGIES

Thanks to communication between the inverters, the same control layer executing the consensus protocol can be used to implement other objectives, not only limited to classical

primary and secondary control objectives. In the consensus-based control, which can converge with power constraints set on the active and reactive power references, the setpoints might be determined by various controllers that are suitable for running in distributed designs. For example, a distributed optimal power flow problem can determine optimal power injections of particular distributed energy resources coupled through the GFD inverters participating in the consensus. The setpoints can be subsequently implemented considering local constraints and measurements. Such strategies are not considered in this work.

III. CYBER-PHYSICAL MODEL

The cyber-physical model is developed to analyze the impact of both cyber and physical layers and the coupling between them on system dynamics and stability. It integrates dynamics of physical, control and communication domains. Physical layer refers to electrical and inverter control equations, while the cyber layer refers to consensus equations, i.e., equations where exchange of information is required. It is important to highlight that unless other work in this area, the presented model is based on the DQ domain, what is a well-known concept in, e.g., inverter control and different types of modelling in power systems. In case of proposed control scheme, DQ domain is considered sufficient since the droop equations are limited only to synchronization between GFM inverters, and modelling of frequency and angles for the purpose of power sharing is not necessary. The frequency is kept at the reference of GFM inverters, and it fluctuates only in transient moments, after which it is restored to the nominal level [24] by the GFM inverters. Through this simplification, the CP model allows easier modelling of larger systems and analysis of larger cyber networks where more complex communication design can be considered.

The impact of different reporting rates from inverters and from metering devices is not investigated in this work. Reporting rate is assumed at least 100 Hz, and therefore, it can be modelled as a continuous flow of measurements, which is still subject to communication latency. The first description of earlier version of this CP model and subsequent results has been published by the same authors in [34].

A. PHYSICAL LAYER

Physical layer of CP model in the analyzed power systems include equations that describe dynamics of lines and loads, GFM and GFD inverters with their internal dynamics and output filters. Equations of CP model in physical layer allows analysis of arbitrary network topology with arbitrary locations of loads and inverters.

Figure 2. depicts generic structure of the internal control in GFM and GFD inverters, while Table 1 presents the physical equations related to these inverter dynamics [4]. The equations are in DQ-domain and include dynamics of internal control related to voltage and current loops, phase locked loop and output LCL filters. GFM inverters do not use PLL as they

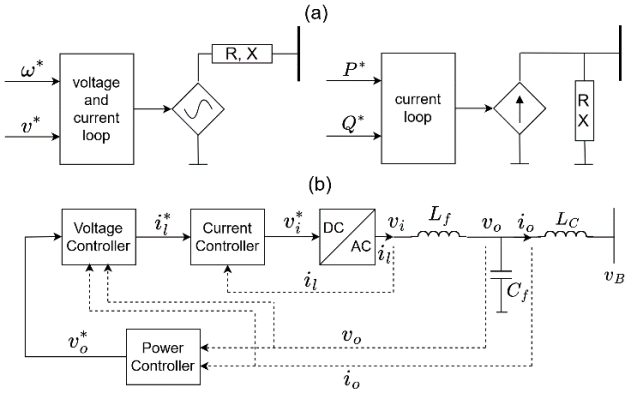

FIGURE 2. (a) Simplified diagram of GFM inverter (left) and GFD inverter (right). (b) Fundamental structure of inner inverter control and its LCL filter.

form the voltage, and the GFD inverters have only current control and no voltage control. Power measurement filtering is applied only to GFM inverters. Internal loops are driven by standard proportional-integral controllers, and output LCL filters connect the inverters to the rest of the network. It is highly recommended for an interested reader to review basic principles of GFM and feeding inverters in [3], [4].

As described in Section II, comparing to the designs in hierarchical control for microgrids, the GFM inverters do not implement the droop for frequency and voltage changes that should govern the power sharing. Instead, the information about the power sharing is communicated to other inverters through cyber layer's communication network. With no synchronization mechanism, the GFM inverters have their internal references of frequency and d- and q-voltages at $v_{od}^* = 1\ p.u.$, $v_{oq}^* = 0$, $\omega^* = \omega_n$, unless the voltage regulation is activated by the consensus control as described in Section III-C2.

Droop-like mechanism is implemented in GFM inverters only for the purpose of synchronization to the network. It is not included for GFD inverter and does not drive the power sharing. The synchronization of GFM inverters in the DQ-domain is realized through equations presented in Table 1, where the difference between locally derived droop variables ω_i is used to control the q-axis reference of the voltage in the voltage control loop of GFM inverters. It is not necessary to consider a delay of the variable ω_j in the local controller, as in the real network, the synchronization occurs based on local measurements. The voltage references of GFM inverters are controlled through the variable V_n^{local}, which is derived based on only local reactive power measurement in order to minimize the infeed by GFM inverters and it contributes to the reference V_n^* together with consensus-based voltage regulation described in Section III-C2.

The dynamics of the network are modelled through the current equations of the lines and loads, similarly in DQ domain. Table 2 includes differential equations describing the dynamics of currents [4]. The electrical connections in

TABLE 1. Physical layer equations I – inverter equations.

Dynamics	Equation
P, Q measurement filters	$P_{mf} = \frac{\omega_C}{s+\omega_C}(v_{od}i_{od} + v_{oq}i_{oq})$ $Q_{mf} = \frac{\omega_C}{s+\omega_C}(v_{oq}i_{od} - v_{od}i_{oq})$
Inverter voltage control	$\dot{\phi_d} = v^*_{od} - v_{od}$ $\dot{\phi_q} = v^*_{oq} - v_{oq}$ $i^*_{ld} = K_f i_{od} - \omega_n C_f v_{oq} + K_{pv}(v^*_{od} - v_{od}) + K_{iv}\phi_d$ $i^*_{lq} = K_f i_{oq} + \omega_n C_f v_{od} + K_{pv}(v^*_{oq} - v_{oq}) + K_{iv}\phi_q$
Inverter current control	$\dot{\gamma}_d = i^*_{ld} - i_{ld}$ $\dot{\gamma}_q = i^*_{lq} - i_{lq}$ $v^*_{id} = -\omega_n L_f i_{lq} + K_{pc}(i^*_{ld} - i_{ld}) + K_{ic}\gamma_d$ $v^*_{iq} = \omega_n L_f i_{ld} + K_{pc}(i^*_{lq} - i_{lq}) + K_{ic}\gamma_q$
PLL of GFD inverters	$\dot{\gamma}_{PLL} = v_{oq}$ $\omega = \omega_n + k_{p\,pll}\,\dot{\gamma}_{PLL} + k_{i\,pll}\,\gamma_{PLL}$
Output LCL filter	$\dot{i_{ld}} = -\frac{R_f}{L_f}i_{ld} + \omega i_{lq} + \frac{1}{L_f}v_{id} - \frac{1}{L_f}v_{od}$ $\dot{i_{lq}} = -\frac{R_f}{L_f}i_{lq} - \omega i_{ld} + \frac{1}{L_f}v_{iq} - \frac{1}{L_f}v_{oq}$ $\dot{v_{od}} = \omega v_{oq} + \frac{1}{C_f}i_{ld} - \frac{1}{C_f}i_{od}$ $\dot{v_{oq}} = -\omega v_{od} + \frac{1}{C_f}i_{lq} - \frac{1}{C_f}i_{oq}$ $\dot{i_{od}} = -\frac{R_c}{L_c}i_{od} + \omega i_{oq} + \frac{1}{L_c}v_{od} - \frac{1}{L_c}v_{Bd}$ $\dot{i_{oq}} = -\frac{R_c}{L_c}i_{oq} - \omega i_{od} + \frac{1}{L_c}v_{oq} - \frac{1}{L_c}v_{Bq}$
GFM synchronization	$\omega_f = \dot{\theta}_f = \omega_n - K^P_f \Delta P_f$ DQ model: $\dot{v}^*_{oq} = K'^P_f(\omega_{fi} - \omega_{fj})$
GFM local voltage reference control	$\dot{V^Q_f} = K^Q_f \Delta Q_f$ $V^*_n = V_n + V^Q_f$

TABLE 2. Physical layer equations –network equations.

Dynamics	Equation
Line currents	$\dot{i}_{line\,ij\,d} = -\frac{R_{line\,ij}}{L_{line\,ij}}i_{line\,ij\,d} + \omega i_{line\,ij\,q} + \frac{v_{Bd\,j} - v_{Bd\,i}}{L_{line\,ij}}$ $\dot{i}_{line\,ij\,q} = -\frac{R_{line\,ij}}{L_{line\,ij}}i_{line\,ij\,q} - \omega i_{line\,ij\,d} + \frac{v_{Bq\,j} - v_{Bq\,i}}{L_{line\,ij}}$
RL loads	$\dot{i}_{load\,L\,d} = \frac{v_{Bd}}{L_{load}} + \omega i_{load\,Lq}$
	$i_{load\,d} = i_{load\,R\,d} + i_{load\,L\,d}$ $\dot{i}_{load\,L\,q} = \frac{v_{Bq}}{L_{load}} - \omega i_{load\,Ld}$ $i_{load\,q} = i_{load\,R\,q} + i_{load\,L\,q}$
Bus voltages	$v_{Bd} = r_N(i_{od} - i_{load\,d} + i_{line\,ij\,d})$ $v_{Bq} = r_N(i_{oq} - i_{load\,q} + i_{line\,ij\,q})$

the network, practically defining the electrical topology in the microgrid, are described through line ends i and j at the bus voltages v_{Bi} and v_{Bj}, while the output currents injected or consumed by the inverter and loads are described through states i_o and i_{load}, respectively, with their sign depending on whether current is injected or withdrawn from the system.

B. CYBER LAYER

In the cyber layer, the devices (GFM, GFD inverters and high reporting rate meters) communicate in distributed consensus manner. Inverters exchange information about active, reactive power references. Measurement devices are installed at some buses in the network, and can only communicate in a unidirectional way, sending its power and voltage measurements to inverters. Phasor measurement units (PMU) are ideal candidates of measurement devices that can provide necessary measurements of active, reactive powers and voltage with high reporting frequency. Therefore, naming of high reporting rate meters is often simplified to PMU in this work.

GFM inverters communicate information about power imbalance, to at least one GFD inverter, what subsequently initiates consensus between GFD inverters. It is important to distinguish that while GFM inverters and PMU meters communicate active and reactive power measurements to other parties, GFD inverters sends active and reactive power references, which are not directly measured powers. Power references account for measurements from PMU meters, as described through the equations in following sections, and allow operation under constraints of output power, not compromising consensus control.

In the subsequent sections, the operation and dynamics of consensus-based controllers are described.

1) CONSENSUS CONTROL

Fundamental dynamics of consensus in a network of distributed elements can be represented by [38]:

$$\dot{x}_i(t) = \sum_{j \in N_i} a_{ij}\left[x_j(t) - x_i(t)\right], x(0) = z. \quad (1)$$

Then the dynamics of the system can be expressed in compact form $\dot{x} = -Lx$, where L is the graph Laplacian defined as $L = D - A$, where D is the degree matrix (of diagraph matrix G with n nodes), with only diagonal elements and zero off-diagonal elements. Thus, in practice, the matrices L, D, A are square matrices of size n that define topology of communication. Additionally, matrices P and G_S define, which inverters receive information from high reporting rate meters, and which inverters receive information from which GFM

inverters. These matrices are used to structure the elements in consensus equations of cyber layers so that the final set of equations accurately represents the communication topology of cyber layer.

The convergence of distributed consensus algorithm as a linear system is asymptotically reached for all initial states if there is a directed path connecting any two arbitrary nodes in the consensus (so-called *strongly connected* graph in graph theory [35]). More systematic way of representing communication topology based on directed graph theory is presented in [36] and [35]. In the presented consensus-based control for microgrids, cyber layer has significant impact on dynamics. The signals X_i, which are communicated in the consensus manner, are not only directly dependent on topology of communication and delay at links τ_{ij}, but also on physical layer dynamics that is described by physical layer state equations. Ultimately, they determine the dynamics of consensus states $\dot{u}_i$:

$$\dot{u}_i = K_i \sum_{j \in N_i} \left[X_j(t - \tau_{ij}) - X_i(t) \right] \tag{2}$$

where: X_i, X_j are values for nodes i and j respectively; communication latency τ_{ij} in the link between nodes i and j; N_i is the set of neighbouring nodes of node i; K_i is the convergence constant. In the equations, the vales, which are not subject to communication delay, i.e., $X(t)$ are often simplified to X for better readability. Further details about consensus control are described in Section III-C.

In the context of studied system, it is important to mention that in case of a communication link failures dividing communication network into independent areas, local consensuses can be also reached, provided the synchronization signals from GFM inverter are provided to each local area. Such operation still provides the main objective of the operation, i.e., reaching the desired output power of GFM inverter and keeping the reserve in the system.

2) COMMUNICATION DELAY

In this study, the reduction of communication latency for the devices in the geographical vicinity are reflected through the so-called edge clouds of the communication network that are often used in the nomenclature of modern communication, where the devices in proximity are connected through the same transmitting hardware. Thus, if the devices are in the same edge of the network, the communication latency between them can be significantly reduced, while if they are not in the same edge network, the communication must happen through a regular network path and the latency is not reduced. The feature of latency reduction between some devices is elaborated by direct assumption of lower delays for the devices in the same edge network, depending on the cyber layer configuration.

C. CONSENSUS IN MG CONTROL

In this section, the operation of distributed consensus controllers is described. In the CP model, the consensus equations are part of the cyber-layer. Steady-state convergence of the control is discussed with respect to cyber- and physical-layers and coupling between them.

1) POWER RESERVE CONSENSUS

As described in Section II, the fundamental operation in consensus control aims maintaining instantaneous power reserve of the microgrids through shifting the power imbalances from response of GFM inverters to the GFD inverters. Such operation is here called power reserve consensus and it does not involve objective of voltage regulation. The interception of power by GFD inverters is subject to propagation of information in the consensus protocol between GFD inverters. The consensus can be additionally supported by active and reactive power measurements from high reporting rate meters (e.g., PMUs). Consensus control of i-th GFD inverter is governed by equations in the cyber layer:

$$\begin{aligned} \dot{P}_i(t) = -K_i^P \Big(\sum\nolimits_{j \in N_i} \left[P_{i\,ref}(t) - P_{jref}\left(t - \tau_{ij}\right) \right] \\ - \Delta P_f (t - \tau_{fi}) \Big) \\ P_{i\,ref}(t) = P_i(t) + K_{\phi m}^P P_{\phi m}(t - \tau_{mi}) \end{aligned} \tag{3}$$

$$\begin{aligned} \dot{Q}_i(t) = -K_i^Q \Big(\sum\nolimits_{j \in N_i} \left[Q_{i\,ref}(t) - Q_{jref}\left(t - \tau_{ij}\right) \right] \\ - \Delta Q_f \left(t - \tau_{fi}\right) \Big) \\ Q_{i\,ref}(t) = Q_i(t) + K_{\phi m}^Q Q_{\phi m}(t - \tau_{mi}) \end{aligned} \tag{4}$$

where: P_i, Q_i are internal states of GFD inverters describing the dynamics of consensus equations for active and reactive, while the P_{iref} and Q_{iref} are the values that are effectively the references for the current loop control and that are subject to being communicated to the neighbor units; τ_{ij} and τ_{mi} are the communication latency values for the link between inverters i and j or between m-th PMU and i-th inverter; N_i is the set of neighboring nodes of node i; K are different convergence constants.

In practice, the P_{iref} values include yet the measurements $P_{\phi m}$ from PMUs. Substituting equations for P_{iref} into the state equations, one can derive that the introduction of power measurements from PMU buses does not change the steady state of the control; however, it impacts the transient dynamics in the consensus convergence process, especially when measurements are available sooner than information propagating through consensus protocol from GFM inverters, which is subject to several delays, including the propagation in the consensus reference values themselves. Considering the modern communication structures, where, due to the physical and cyber proximity, measurements can be available sooner, convergence can be improved. Different scenarios are considered in Section V.

Use of reference values in the consensus protocol instead of real measured values is determined by the operation under constrained active or reactive power output. Such constrains exist due to installed rated powers of the inverters but may also appear due to limited power of the battery or state of charge (SoC) of the battery in combination with some forecast

algorithms. Constraints can be tightened to single values for P and Q reference points in case it is necessary that some GFD inverters feed precisely a desired amount of power irrespective of the consensus control setpoints. In situation of constrained output, when measured values are used directly, consensus protocol would not be able to converge. On the other hand, using the reference values can decrease the accuracy of the power infeed. Inaccuracy of this type can be mitigated with improvements in internal inverter controllers.

Eq. 3-4 for P_i and Q_i states are directly the linear consensus equations like Eq. 1. Moreover, the devices participating in the consensus (GFD inverters) can actively regulate their P and Q outputs, therefore a global solution, provided the fulfilment of basic consensus convergence principles explained in Section III-B, and assuming unconstrained power infeed, always exists for power reserve consensus.

2) VOLTAGE CONSENSUS

Voltage consensus aims maximization of active power reserve through distributing the power references among GFD inverters (same to the power reserve consensus, but with active power only), and simultaneously the regulation of voltage through the consensus between buses participating in the consensus control, i.e., (i) voltages at the output buses of the GFD inverters and (ii) voltages from buses without dispatchable units, but where high reporting meters are installed and supply measurements. Such operation aims removing the voltage differences between these buses. As explained in Section II, voltages are more significantly dependent on reactive power flow; therefore, the consensus regulating the voltages is coupled with the equations for reactive power references Q_i, while the active power is governed through Equation 3 from power reserve consensus.

$$\begin{aligned}\dot{Q}_i(t) = -K_i^V \Big(&\sum\nolimits_{j\in N_i}\left[V_i\left(t\right) - V_j\left(t-\tau_{ij}\right)\right] \\ &+ \sum\nolimits_{j\in M_i}\left[V_i\left(t\right) - V_{\phi m}\left(t-\tau_{mi}\right)\right] - \delta v_i\Big) \\ Q_{i\,ref}(t) = Q_i(k) &+ K_{\phi m}^Q Q_{\phi m}(t-\tau_{mi})\end{aligned} \tag{5}$$

One can see that in the Equation 5, the first sum component represents voltage consensus between the bus voltages V_i, V_j of GFD inverters, while the latter the consensus between buses of inverters V_i and the buses with voltage measurements supplied by high reporting rate meters $V_{\phi m}$. In the Eq. 5, there is no information supplied by GFM inverter, only voltage references exchange between the GFD inverters supported by voltage and reactive power measurements from PMUs.

Non-dispatchable buses cannot regulate their active and reactive power infeed, thus also their own voltage. Therefore, voltages of non-dispatchable buses are strongly dependent on voltages at the neighbor buses. It is related to the dynamics of the physical layer, especially to the impedances between dispatchable and non-dispatchable buses, therefore the consensus with non-dispatchable buses can be limited on the convergence, especially in case of strict requirements on accuracy of the consensus. Relaxation of the voltage precision is introduced by component δv_i in Eq. 5, in order to help with the convergence of the voltage consensus, decreasing its accuracy. It is considered in the designed control especially for the consensus with one or more non-dispatchable buses.

Due to strong coupling (dependence) of voltage consensus to the physical layer, even when the convergence is provided, the voltage profiles might be violating the limits, for example due to the physical features of the network, such as high R/X ratio, but also in case of limited availability of reactive power. It might be then necessary to involve GFM inverters in the voltage consensus control, using their capability to globally modify voltage references. In this way, the shift of voltages in entire microgrid is possible. In the operation, the most deviated voltage in the consensus protocol V_j is controlled by the GFM inverters through the equations:

$$\begin{aligned}V_n^* &= V_n + V_f^Q + V_f^C \\ \dot{V_f^C} &= K_f^V\left(V_j\left(t-\tau\right) - V_{low}\right)\end{aligned} \tag{6}$$

wher: V_n^* is the adjusted reference voltage of GFM inverter, which is modified by state V_f^C. V_f^Q is the locally driven state described earlier in Table 1. Effectively, the GFM inverters make the voltage from the consensus protocol V_{cons} converge to the desired level of V_{low}, what propagates to the other voltages (governed by reactive power consensus) participating in the consensus control. Differently to power reserve consensus, the voltage consensus in the cyber layer becomes nonlinear since it is more dependent on physical layer described by nonlinear equations for currents and voltages. Therefore, the linearization of the voltage consensus and thus its small-signal stability analysis can become much less accurate.

3) COMBINED CONSENSUS OPERATION

The combination of the power reserve and voltage consensus control from previous subsections is considered when the reactive power equations Eq. 4 and Eq. 5 are combined to drive the dynamics of reactive power reference:

$$\begin{aligned}\dot{Q}_i\left(t\right) = -K_i^Q \Big(&\sum\nolimits_{j\in N_i}\left[Q_{i\,ref}\left(t\right) - Q_{jref}\left(t-\tau_{ij}\right)\right] \\ &- \Delta Q_f\left(t-\tau_{fi}\right)\Big) \\ &- K_i^V\Big(\sum\nolimits_{j\in N_i}\left[V_i\left(t\right) - V_j\left(t-\tau_{ij}\right)\right] \\ &+ \sum\nolimits_{j\in M_i}\left[V_i\left(t\right) - V_{\phi m}\left(t-\tau_{mi}\right)\right] - \delta v_i\Big) \\ Q_{i\,ref}(t) = Q_i(k) &+ K_{\phi m}^Q Q_{\phi m}(t-\tau_{mi})\end{aligned} \tag{7}$$

It is considered a more practical solution because the control of active, reactive power and voltage might be necessary at the same time. The ratio of coefficients K_i^V/K_i^Q determines the accuracy of bus voltages and accuracy of reactive power infeed (thus amount of Q reserve) in the consensus control. The coupling between Q and V consensus has similar positive effect for voltage consensus relaxation as the introduction of relaxation component δv_i, i.e., better steady-state convergence of the control for operation with higher R/X

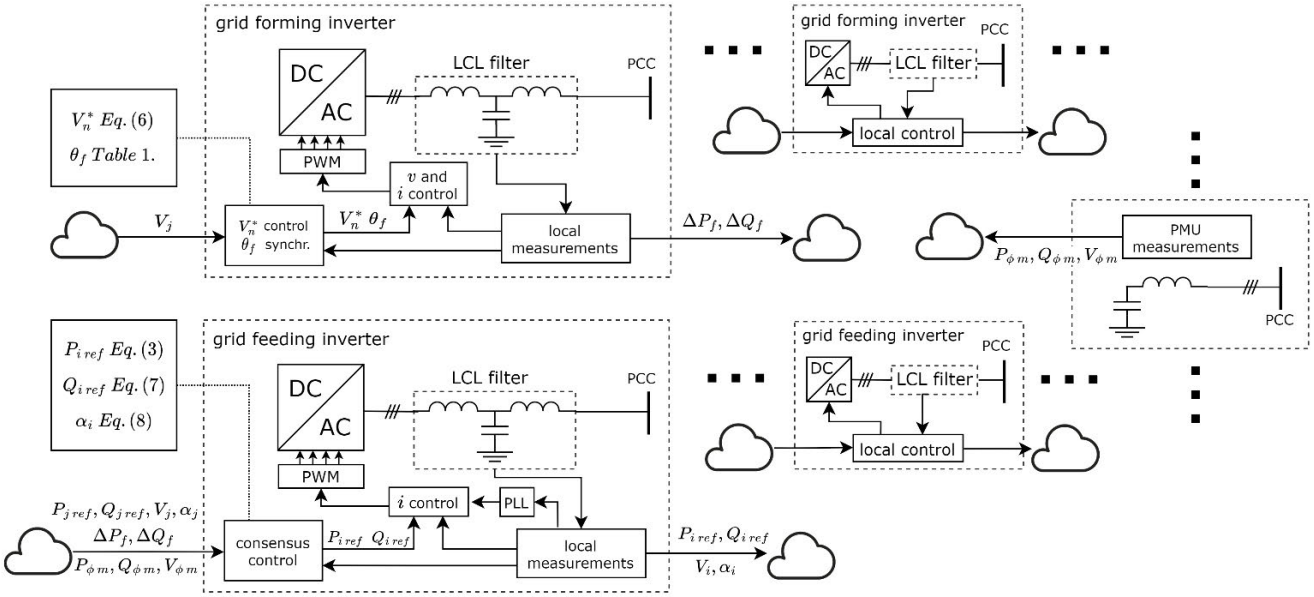

FIGURE 3. Flow chart diagram of the MG control scheme with grid forming, feeding inverters, and high reporting rate meters (PMU measurements).

ratio. In practice, better steady-state convergence is achieved through less accuracy in the reactive power consensus.

As described in Section II, the operation aiming maximization of active and reactive power reserve is considered the default operation mode, when other constraints are not violated. In the combined consensus operation, the default operation is achieved through low K_{Vi}/K_{Qi} ratio, which prioritizes reactive power consensus over voltage consensus in the Eq. 7. The support from active and reactive power measurements of high reporting rate PMUs can be active continuously, as its purpose is to improve the dynamics during the transients.

In case the voltage levels of the buses participating in the consensus are violated, the voltage consensus regulation is initiated. First, when the GFM inverters are involved in the consensus, the voltage measurements of dispatchable or non-dispatchable buses involved propagate to them in the consensus protocol. The GFM inverters are then able to apply Eq. 6 and modify their voltage references as described in the previous subsection. Other voltages are also shifted since they are coupled through voltage consensus control.

Secondly, in case of voltage violation, the ratio K_i^{V}/K_i^Q is locally adjusted by GFD inverters in order to increase the weight of the voltage control in the Q_i consensus according to the Eq. 8.

$$\begin{aligned}\dot{\alpha}_i(t) &= -K_i^{\alpha}\left(\sum\nolimits_{j\in N_i}\left[\alpha_i(t)-\alpha_j\left(t-\tau_{ij}\right)\right]-\Delta V_i(t)\right)\\ \Delta V_i &= V_i(t)-V_{high}\\ K_i^V &= K_{0i}^V+\alpha_i\end{aligned} \tag{8}$$

With higher K_i^V and thus higher K_i^{V}/K_i^Q ratio, part of the reactive power reserve is used then for the voltage control. Through the consensus protocol, the values α_i adjust K_i^{V}/K_i^Q for each GFD inverter in the consensus manner. In practice, the unit with the most extreme, e.g., highest voltage level among the units participating in the consensus, violating the voltage level V_{high} first, adjusts its own coefficient and thus initiates the consensus with other units.

In the Figure 3, one can see the diagram that describes information flow in the presented control scheme, where GFM, GFD inverters and high reporting rate units exchange references and measurements (realizing the combined operation with both power reserve and voltage consensuses as described in this section).

D. OPERATION UNDER COMMUNICATION DELAYS

Due to strong dependence of the control on the communication and cyber layer, effect of different delays is assessed. As described in Section III-B2, communication latency and thus, delays in different edge clouds can be different to delays in the same edge cloud.

It is important to check first whether the control has a solution, i.e., it converges for assumed topology, physical features, consensus coefficients and relaxation. Then, the assessment of the operation under delays in cyber layer can define further boundaries on the cyber and physical layer design. The operation under delays can be evaluated through nonlinear numerical solution of the full CP model with the cyber and physical layer equations presented in the previous sections. So-called pseudospectral approach is used for the CP model in order to assess small-signal stability of consensus control operation under multiple communication delays. It can evaluate stability of linear systems, therefore the full nonlinear CP model has to be linearized.

The pseudospectral approach is based on [37], [38], where system of DDE is described as:

$$y'(t) = f(y_t)$$
$$f(\varphi) = \sum_{l=0}^{k} L_l \varphi(-\tau_l) + \int_{-\tau}^{0} M(\theta)\varphi(\theta)\,d\theta, \varphi \in X \quad (9)$$

Given a positive integer N, we consider Ω_N is a set of $N+1$ distinct delay points:

$$\Omega_N = \{\theta_{N,i}, i = 0, 1, \ldots, N\} \quad (10)$$

It is derived [37], [38] that the problem of a system of DDE is turned into the eigenvalue problem for the so-called spectral differentiation matrix A_N, i.e., the eigenvalues of A_N directly approximate the characteristic roots of original DDE problem and can be summarized in the following form [39]:

$$A_N = \begin{bmatrix} \hat{C} \otimes I_n \\ A_{\tau max}\ \ 0\ldots0\ A_2\ 0\ldots0\ \ A_1\ 0\ldots0\ A_0 \end{bmatrix} \quad (11)$$

where: $\hat{C}$ is the matrix of first $N-1$ rows of $C = -2D_N/\tau$, D_N is the Chebyshev's differentiation matrix of order N. N is chosen according to maximum delay and desired accuracy discretizing delay into desired number of equal parts. In this work it is assumed that the fundamental delay interval equals 10 ms, therefore in case of analysis of a case with maximum delay of 200 ms, N equals 20, and there would be 20+1 sub-matrices A for delays of 0, 10, 20, …, 190, 200 ms. The accuracy analysis of such approach is presented in [37].

In case of fundamental operation of power reserve consensus aiming maximization of power reserve, the stability is significantly dependent on cyber layer, that is, on P_i, Q_i states. The selective modal analysis (SMA) additionally reveals that the dominant participation factors for the modes come indeed from P_i, Q_i states of the cyber layer. The linearized model gives therefore a good accuracy assessment of the small-signal stability under multiple delays.

In case of consensus for voltage regulation, the equations describing voltages are nonlinear and strongly related to the physical layer; therefore, the linear model is less accurate for the assessment of small-signal stability. Therefore, a simplified 2-bus model is derived, which provides good accuracy when analyzing convergence and operation under delays of voltage consensus with a non-dispatchable bus. In this model, the system with voltage consensus before considering a new bus is aggregated to a single GFD inverter connected to bus with V_{cons} (Fig. 4), and it is then analyzed with a new bus joining the consensus control (V_{new}). In this way, the model is reduced to 9 states and the small-signal stability results give sufficiently accurate results (comparing to nonlinear model) when investigating impact of different coefficients and delays, in a bus-by-bus analysis.

In this work, through the pseudospectral approach (Eq. 9-11), result of analysis of the fundamental operation of consensus controlled islanded microgrid are presented, that is, when the voltage consensus is minimized, and the dynamics are driven by the power reserve consensus.

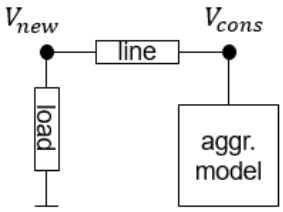

FIGURE 4. Two-bus aggregated model for small-signal analysis of voltage-consensus with non-dispatchable buses.

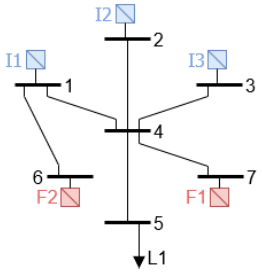

R_{L14}, X_{L14}	3.291, 3.222
R_{L24}, X_{L24}	7.884, 5.357
R_{L34}, X_{L34}	1.462, 1.432
R_{L61}, X_{L61}	0.454, 0.363
R_{L74}, X_{L74}	3.291, 3.222
R_{L45}, X_{L45}	2.7, 0.363

FIGURE 5. 7-bus test system topology and line data.

TABLE 3. Default system parameters for both 7- and 28-bus systems.

Parameter	Default value
Delay	120 ms
Edge cloud delay	15 ms
Nominal voltage (V_n)	11 kV
Nominal frequency (ω_n)	100π Hz
Power filter frequency (ω_c)	1000π $1/s$
I control coeff. (K_f, K_{pc}, K_{ic}) – g. forming	0.2, 0.2, 125
V control coeff. (K_{pv}, K_{iv}) – g. forming	0.2, 125
I control coeff. (K_{pc}, K_{ic}) – g. feeding	0.2, 125
PLL parameters	1e-3, 1e-4, 0
LCL filters parameters (R_f, L_f, C_f, R_c, L_c)	1e-3, 1e-4, 1e-5, 1e-3, 1e-4
Parameter r_n	$1e3$
Default consensus coefficients (k_{p1-5}, k_{q1-5})	3, 3

IV. TEST SYSTEMS

Two test systems are considered. A 7-bus MV microgrid system with two GFM and three GFD inverters is used to observe details of the dynamics in proposed consensus control operation. Subsequently, a 28-bus MV system is used to examine some phenomena that are distinct for larger cyber-physical system.

A. 7-BUS TEST SYSTEM

The 7-bus MV system includes 2 GFM inverters, 3 GFD inverters, 5 lines and a single load. In the smaller system the basics of the operation are clearer as many dynamics are coupled. With these elements, full cyber-physical model has 80 states, 69 from physical layer (including 28 related to GFM inverters, 27 to GFD inverters and their output filters) and 11 from cyber layer (including 9 for consensus control

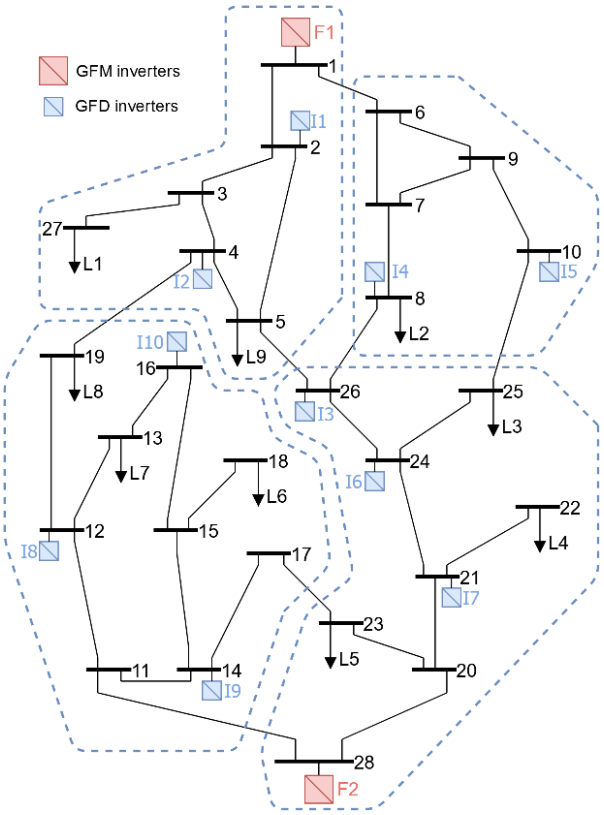

FIGURE 6. 28-bus test system topology.

between GFD inverters and 2 for voltage regulation of GFM inverters). R/X ratio in the system is between 1.02 and 1.47 as one can see in the Figure 5. and Table 3.

B. 28-BUS TEST SYSTEM

A larger 28-bus MV system from [40] is implemented for the tests so that the impact of communication and edge cloud structure can be distinguished. It consists of 28-buses at medium voltage, 2 GFM and 10 GFD inverters, 9 parallel RL-impedance loads and 34 lines with R/X ratio between 1.02 and 1.56. With this configuration, full cyber-physical model has 236 states, 204 from physical layer (including 118 related to inverters and their output filters) and 32 in cyber layer. Figure 6 depicts the physical network of the 28-bus system.

In the 28-bus system, 4 edge clouds are indicated (blue dashed lines), which are analyzed in different configurations. The communication latency within the edge cloud is reduced thanks to the geographical proximity. As the result, in the 28-bus system one can observe operation with consensus control scheme supported by PMU, similar to the 7-bus system, but focused on comparison of 4 cases of edge cloud (cyber layer) design.

V. RESULTS

The results are presented in the scenarios that expose main operation principles of control scheme with its objectives as

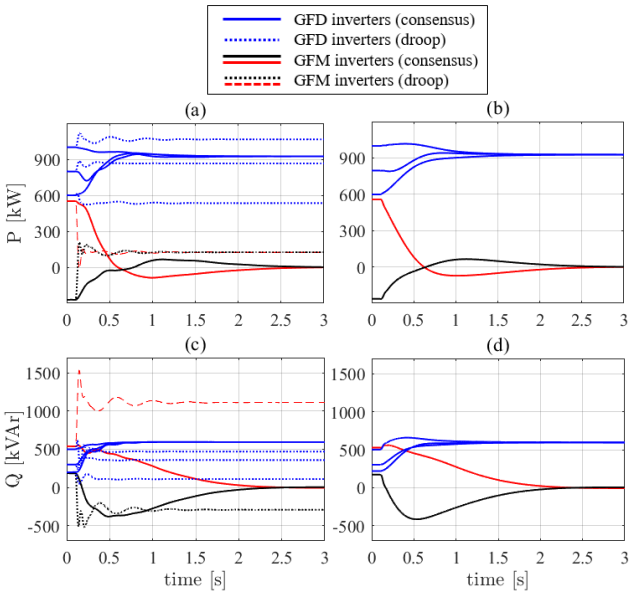

FIGURE 7. Fundamental operation of the consensus control aiming maintaining active (a b) and reactive (c d) power reserve.

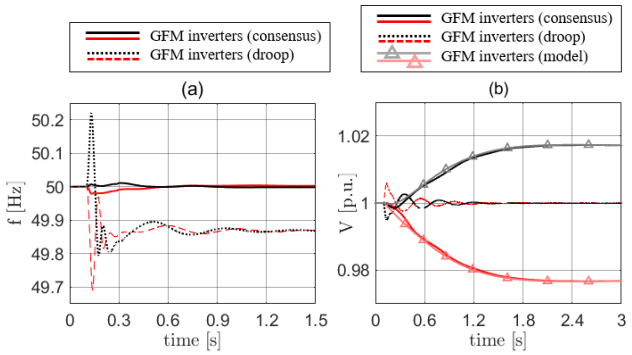

FIGURE 8. Fundamental operation of the consensus control aiming maintaining power reserve: responses of frequency (a) and voltage (b) at buses with GFM inverters.

described in Section II and III. The dynamics of complete system (when using power reserve and voltage consensus supported by PMU measurements) is presented, also assessing coupling between physical- and cyber-layer and impact on steady-state convergence. Results of the scenarios in the test system consist of time-domain solutions of the CP model, calculated in MATLAB by different solvers and in Simulink and results of small-signal analysis through pseudospectral approach.

A. POWER RESERVE CONSENSUS

Proposed consensus control scheme for islanded MG realizes its GFM inverters power reserve maximization operation through power reserve consensus, as described in Section III-C1. This mode of operation is presented in the Figures 7. and 8., where before $t = 0.1$s, power reserve consensus is not active and GFD inverters operate with fixed

setpoints. At $t = 0.1$s, the consensus control is activated and the GFD inverters start to overtake the active and reactive power infeed of GFM inverters. In this way, the objective of GFM inverters power reserve maximization is realized, effectively unloading the GFM inverters. Voltage consensus control is not active.

The operation of power reserve consensus in the control scheme can be compared to the droop control (dashed lines) in the Figures 7ac and 8. One can see the drawbacks of the droop control where a non-nominal steady state of frequency appears, while the operation points for GFM and GFD inverters are according to the predefined droop curve, not necessarily at a desired and not controllable without a secondary control. The frequency RoCoF and nadir are also significantly higher for operation with droop. The voltages of GFM inverters (Figure 8b) are regulated by states V_f^Q (Table 1) in order to minimize the reactive power infeed of GFM inverters and maximize their reserve. The time to reach steady-state for both methods is comparable, with slightly faster droop dynamics for the presented case ($\sim$ 1.5s vs. $\sim$ 2.5s).

In the Figure 7, the curves of a full EMT 3-phase model (Figures 7ac), can be compared with those from DQ-domain cyber-physical model (Figure 7bd) proposed in this study. One can see similar responses in both models, with the difference of missing dynamics of active power synchronization (through GFM inverters droop equations) in the DQ-domain model. This dynamic is however not crucial for stability in the entire system, and it is not driving the power sharing in the MG, therefore one gets much more flexibility on its adjustment for each GFM inverter to avoid unwanted behavior.

The consensus control is described through the equations Eq. 3 and Eq. 4. and it needs communication network providing propagation of the power references. The cyber layer is configured in the way that communication matrix for 7-bus system with 3 GFD inverters (as described in section III-B1) are:

$$A = \begin{bmatrix} 0 & 1 & 0 \\ 1 & 0 & 1 \\ 0 & 1 & 0 \end{bmatrix} G_s = \begin{bmatrix} 1 & 0 & 0 \\ 0 & 2 & 0 \\ 0 & 0 & 1 \end{bmatrix} P_S = \begin{bmatrix} 0 & 0 & 0 \\ 0 & 0 & 0 \\ 0 & 0 & 1 \end{bmatrix}$$

They represent communication topology where e.g. the 2$^{\text{nd}}$ inverter (second row in matrices above) communicates with two neighbor inverters 1$^{\text{st}}$ and 3$^{\text{rd}}$, and only the 3$^{\text{rd}}$ inverter receives P, Q imbalance signals from both GFM inverters (third row in P_S). The signals are subject to default delays as described in Table 3. The bus voltages are within the assumed safe boundaries of 0.85 and 1.15 p.u. and thus, voltage regulation is not active.

In the Figure 9., one can see the comparison between four cases when consensus control is supported by high reporting rate meters like PMUs. The meters publish voltages, active and reactive power measurements at bus 5, where load is located. The local controllers of GFD inverters receives the measurements and use them in the control ($P_{\phi m}$ and $Q_{\phi m}$ in Eq. 3-4) impacts their power reference and effectively

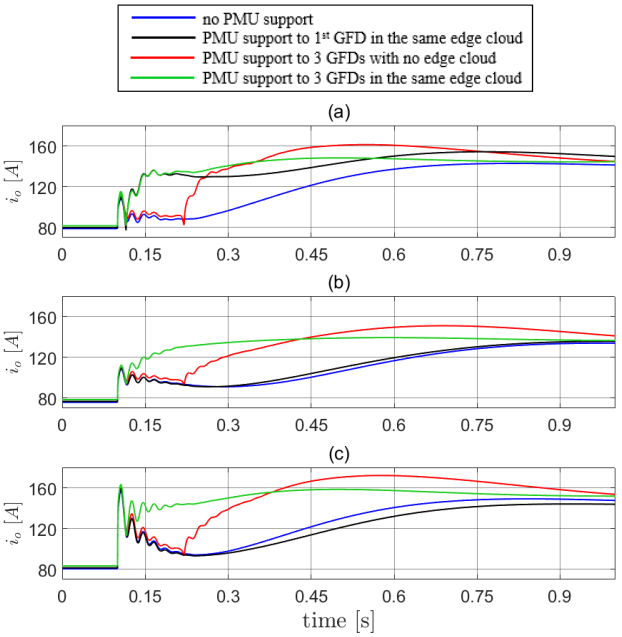

FIGURE 9. GFD inverters' output current responses with different high reporting rate meters (PMUs) configurations.

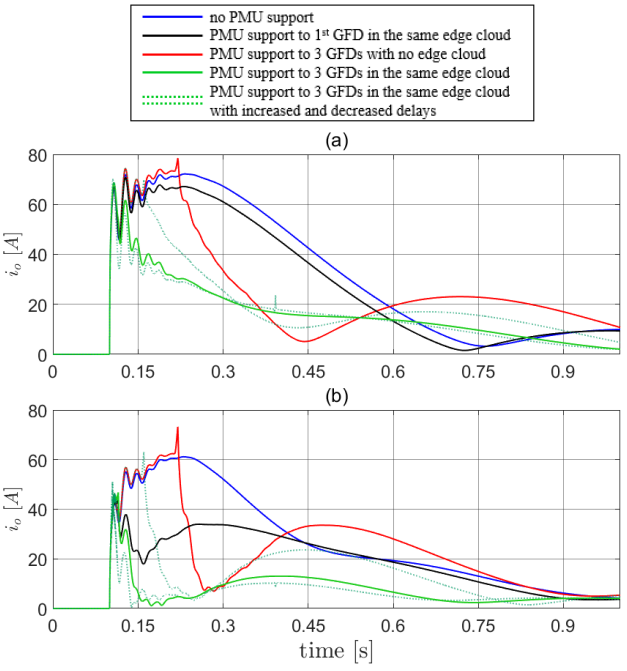

FIGURE 10. GFM inverters' output current responses with different high reporting rate meters (PMUs) configurations.

the dynamics of GFD inverters. The support is particularly beneficial if the devices are in the same edge cloud (with reduced delay) with one or more GFD inverter. The effect can be further improved when the measurements are sent to multiple GFD units. The four cases differ in term of PMU measurements availability (to 1 or 3 inverters), under regular or edge cloud communication conditions. One can see that

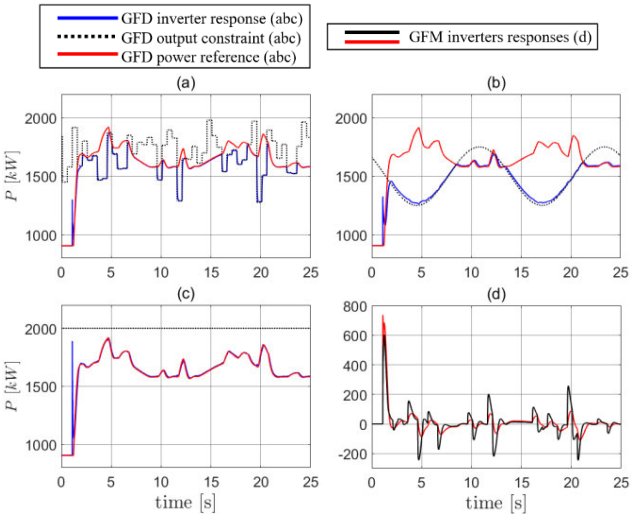

FIGURE 11. Operation of GFD and GFM inverters under constrained active power infeed.

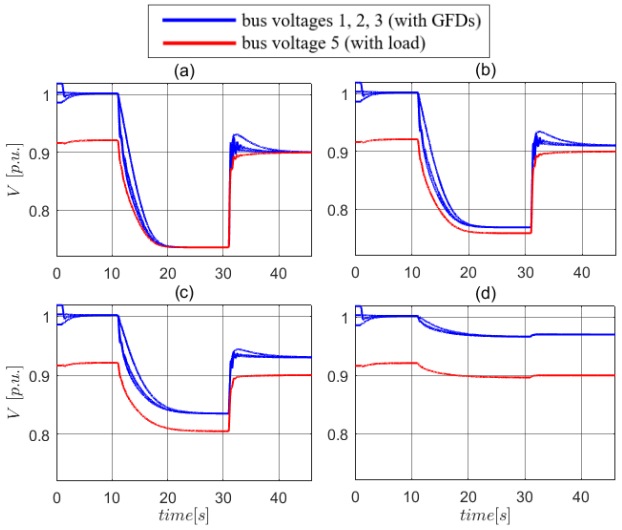

FIGURE 12. Voltage consensus operation with different relaxation parameters δv_i and including GFM inverters controlling the voltage.

the best convergence can be obtained when measurements are available to all GFD inverters with reduced delay.

In the Figure 10., output currents of GFM inverters are presented for the same cases. The fundamental purpose of the operation is to maintain the reserve of GFM inverters; therefore, it is important to improve transient current responses of GFM inverters through additional measurements (to GFD inverters). In the presented configurations of PMU support, one can see that in the scenario with PMU measurements supporting the operations at the edge of the communication network, the GFD inverters (Fig. 9) can converge to their new steady state much faster, and this determines GFM inverters (Fig. 10) to converge faster. The peak of transient current of one of the GFM inverters is significantly reduced, especially for cases in the same edge cloud. It can be observed that support of only one GFD inverter can already significantly improve the response of GFM inverter (F1) that is close to the GFD inverter (I1) supported by PMU measurements (Fig. 10b, black curve).

In the Figure 11, one can see the power reserve consensus operation, but under constrained output of GFD inverters in terms of available active power infeed. The design of the consensus control based on the reference values instead of measured ones enables continuous operation also under power constraints. The responses of GFM inverters (Fig. 11d) show that the GFM units operate as balancing units in a situation of new constrains appearing, similarly to a situation of a disturbance.

B. VOLTAGE CONSENSUS

This section describes voltage consensus operation as described in Section III-C2. In the Figure 12, after $t = 1$s, one can see the voltage consensus of three dispatchable GFM inverters in 7-bus system, which successfully converge to a precisely same level of the voltage at 1 p.u. All three inverters have flexibility of feeding reactive power according to the setpoints derived, though that they are shaping voltage at its output buses. After $t = 10$s, voltage consensus includes bus 5 with RL load that is by high reporting rate PMU. The bus 5 does not include dispatchable units and in such case, the GFD inverters have to provide the reactive power infeed leading all four voltages to converge to the same level (Fig. 12a). As one can see, the convergence of the voltage consensus control for such conditions only happens at the voltage level much lower than operational limits. That is due to the coupling of consensus control to the physical layer, namely the dependence of bus 5 voltage from other voltages through physical line impedances (equations in Table 2). Figures 12b, c, d show the result of the control if the voltage consensus is introduced with the relaxation parameter δv_i described in Section III-C2. One can see that it is then possible to include the voltage of non-dispatchable bus in the voltage consensus that is not causing significant change of the voltage levels at all buses participating in the voltage consensus, at the same time allowing a difference (relaxation) between bus voltage levels.

Due to the strong coupling to the physical layer between the voltages participating in the cyber layer's consensus, one can observe margins of convergences of the voltage consensus operation, for the cases when buses with no dispatchable resources are included. It is strongly related to the R/X of the lines and the parameter of relaxation. Fig. 13 depicts the dependence of convergence of the control with voltage consensus with respect to the R/X ratio of the lines in the network. One can see the stable and unstable region, where the consensus control cannot converge. This aspect has to be strictly considered when designing such control. As the physical features of the network usually cannot be changed, the most reasonable solution is to design the δv_i and other parameters accordingly. Similar effect of relaxation can

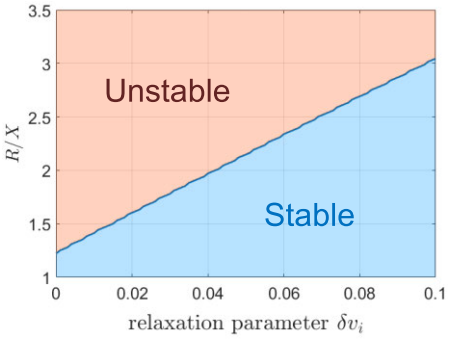

FIGURE 13. Stability margins under different voltage consensus relaxation parameter with respect to R/X ratio.

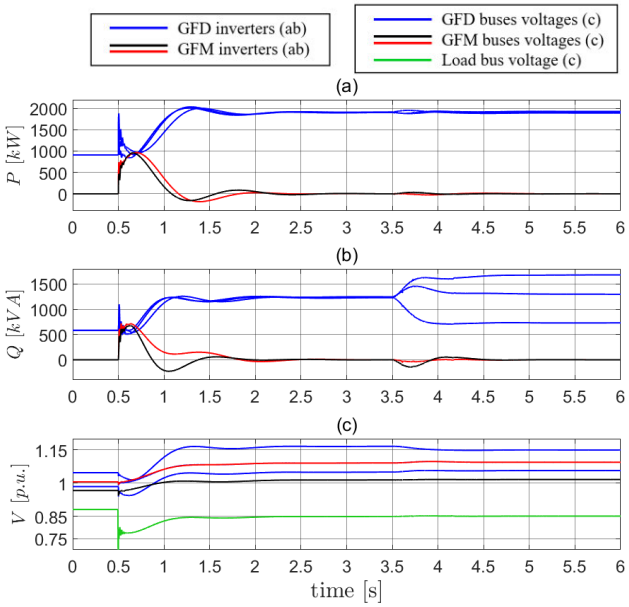

FIGURE 14. Combined consensus operation including voltage regulation by GFM inverters.

be achieved through combining the voltage consensus with power reserve consensus as described in Section III-C3 and presented in the following section.

When the GFM inverters are participating in the voltage consensus through Eq. 6, their task is to maintain e.g. the lowest voltage within the boundaries as described in Section III C4. It might be especially necessary when non-dispatchable buses are involved in the consensus, i.e., when the voltage control is the most difficult. In the Figure 12, after $t = 30$s, the GFM inverters start to control their reference voltage to restore the lowest one in the consensus control (bus 5) to the desired level of 0.9 p.u. As the result, the control converges with the bus voltage profiles closer to each other (depending on the parameter δv_i in different cases) and not violating the lower voltage limit.

C. COMBINED CONSENSUS OPERATION

In the combined operation, as described in Section III C4, the primarily goal of the inverters is to keep power reserve

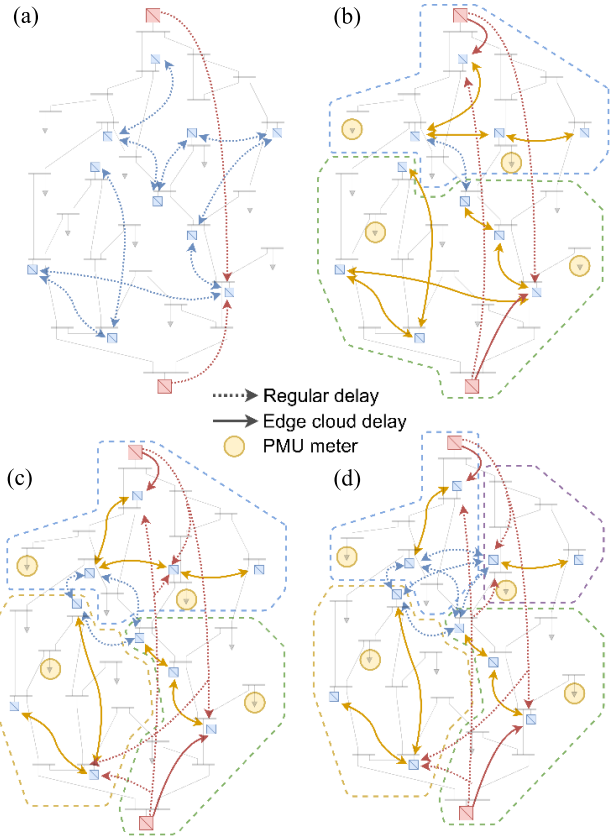

FIGURE 15. Four cyber-layer design cases with different edge clouds (dashed lines polygons) and associated regular and edge cloud delays, based on Figure 6 physical-layer.

consensus. When the voltages of buses in the consensus are violated, the GFM inverters should regulate its voltage reference, and if the voltages of GFD inverters are also violated, they act themselves by increasing their voltage consensus weight in the distributed way through parameters α_i. When combining the Q and V consensus together as described by Eq. 5., the effect of relaxation can be achieved similarly to relaxing directly the voltage consensus through δv_i parameter. The trade-off between voltage and reactive power consensus depends on the ratio of coefficientsyK_{Vi}/K_{Qi} as described in Section III-C3.

In the Fig. 14, at $t = 0.5$s the load increases with the GFM voltage regulation active, what makes the GFM inverters shift the lowest voltage (bus 5) to the minimum level of 0.85 p.u. At $t = 3.5$s, the operation of voltage consensus of GFD inverters is activated and the GFD inverters start to prioritize the voltage consensus in the active power regulation what make them dispatch reactive power differently. In case of presented unconstrained case it is not an issue for GFD inverters; however, the amount of necessary reactive power can be large in case of significant voltage violation.

As the result, the voltages of GFD inverters are getting back to the voltage boundaries at 1.15 p.u., however this happens for the price of change in reactive power sharing

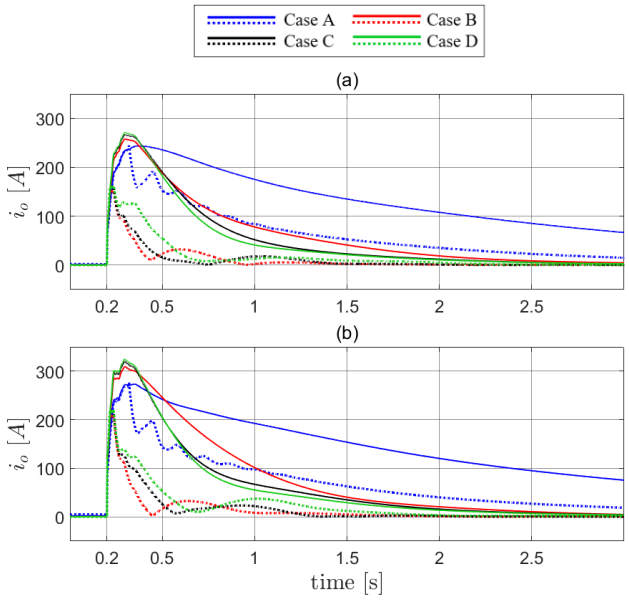

FIGURE 16. Output current responses of GFM inverters, (a) and (b), for four cases of edge clouds designs (from Fig. 15): without PMUs' support (solid lines) and with PMUs' support (dashed lines).

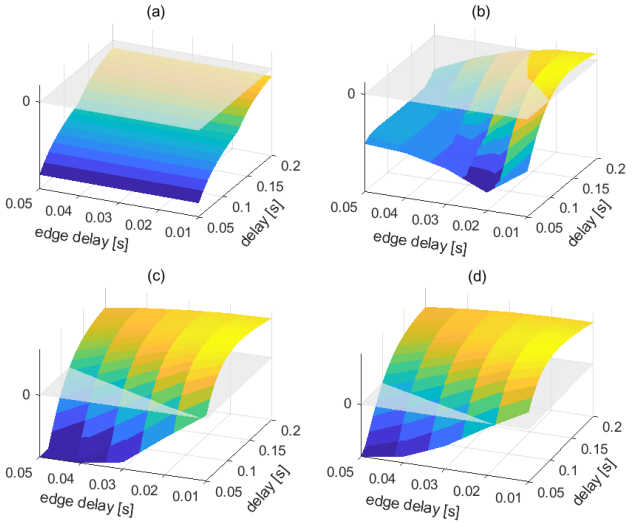

FIGURE 17. Stability margins (gray surface) of four edge cloud design cases with respect to regular and edge communication delays.

accuracy. Thanks to regulation of the local voltage by GFM inverters, the reactive power reserve is again maximized after the changes. The active power reserve is also maintained after transients.

D. EDGE CLOUDS DESIGN

In the 28-bus system, thanks to larger cyber layer with multiple communication nodes and links, we can focus on impact of cyber layer features such as edge cloud design.

We compare 4 cases of different edge clouds for the same physical network (Figure 15).

In the Figure 16., one can see the responses of two GFM inverters in 4 different cyber-clouds designs (solids lines). It is distinguishable from the simulations that the slowest response one gets with Case 1 with no edge clouds. When there is 2,3 or 4 edge clouds that allows reduction of the delay between the inverters inside the edge, the dynamics changes and converges more quickly for all 3 cases with edge clouds Such operation cases have different responses; however, lower peak currents are not guaranteed. When consensus is supported by PMU meters installed (subject to regular delay in case 1 and edge cloud delays in other case), the peak currents can be reduced, and convergence enhanced. In the presented cases, PMU send their measurements to closest GFD inverters, with the same communication topology for all cases. From such analysis, one can design and optimize where PMUs should be installed to improve transient response and speed up the convergence.

Through the pseudospectral approach analysis with multiple delays as described in Section III-D, the operation of power reserve consensus is analyzed for the same four cases. Stability margins of operation under regular and edge cloud delays are presented in the Figure 17, where stable cases are below the 0-surface and unstable above, depending on regular and edge cloud delays.

From response dynamics of GFM output currents and analysis of the delays in the cases, one can observe how the edge clouds can improve the transient response and consensus convergence with and without high reporting rate PMUs, where generally the larger edge clouds with more links of reduced delay provide faster current response, especially with PMUs supporting the operation.

The design of edge clouds in the cyber layer determines different marginal delays guaranteeing stability as depicted in the Figure 17. It can be observed that particular design of edge cloud, which allows faster response (Fig. 16) can on the other hand lead to reduced margins for small-signal stability.

VI. CONCLUSION

In this paper, distributed consensus control for inverter-based islanded microgrids supported by measurements from high reporting rate meters like PMUs is formulated and analyzed for microgrids with grid forming and grid feeding inverters. The control aims maintaining power reserve while keeping the power balance and regulating bus voltages. The study is performed on the formulated cyber-physical model in DQ-domain, analyzing multi-bus microgrids of arbitrary physical and cyber structures and considering edge clouds. The coupling between cyber and physical layer for steady-state convergence and small-signal stability under multi-layer communication is analyzed.

The results acknowledge that the formulated communication dependent distributed consensus for inverter-based systems supported by high reporting rate meters fulfills the objectives of classical hierarchical microgrid control. Operation based on communication-based consensus controller is effective, including accurate power sharing and considering trade-off in reactive power and voltage control,

where the dispatchable devices are able to modify their control objectives in the distributed way. The use of high reporting rate meter devices improves transient response, especially when the measurements devices are placed at the same edge cloud of the communication network. Additional measurements enable also to achieve voltage control for the non-dispatchable buses without inverters. Presented consensus-based control can reach convergence and operate accurately also under constrained output of inverters.

The developed CP model allows for the analysis of dynamics in arbitrary microgrids. The investigation of cyber and physical layers in the operation reveals coupling between the cyber and physical layers and its significant impact on the steady-state convergence of consensus control. The inherent communication in distributed consensus control and communication design implies dependence of network dynamics from cyber-layer (which defines exchange of communicated signals), but also dependence from physical layer. Effectively, the control based on linear consensus in cyber layer becomes nonlinear when it involves dynamics of physical layer. Impact on convergence of both cyber and physical layer should be jointly addressed when designing the operation especially with respect to impedance parameters of the lines and relaxation of the consensus objectives that can improve the convergence of the system control without violation of other constraints.

Impact of different structures of the cyber layer, including the edge clouds reducing some delays is analyzed and reveals marginal delays allowed for stable operation with different cases of cyber layer edge cloud designs. The results acknowledge a trade-off between stability, which is subject to communication latency, and currents' dynamics, i.e., convergence performance. These issues should be carefully addressed in the design process for both physical- and cyber- layers configuration and considering dynamics from both layers jointly.

REFERENCES

[1] J. M. Guerrero, J. C. Vasquez, J. Matas, L. G. de Vicuna, and M. Castilla, "Hierarchical control of droop-controlled AC and DC microgrids—A general approach toward standardization," *IEEE Trans. Ind. Electron.*, vol. 58, no. 1, pp. 158–172, Jan. 2011.

[2] J. M. Guerrero, M. Chandorkar, T.-L. Lee, and P. C. Loh, "Advanced control architectures for intelligent microgrids—Part I: Decentralized and hierarchical control," *IEEE Trans. Ind. Electron.*, vol. 60, no. 4, pp. 1254–1262, Apr. 2013.

[3] J. Rocabert, A. Luna, F. Blaabjerg, and P. Rodríguez, "Control of power converters in AC microgrids," *IEEE Trans. Power Electron.*, vol. 27, no. 11, pp. 4734–4749, Nov. 2012, doi: 10.1109/TPEL.2012.2199334.

[4] N. Pogaku, M. Prodanovic, and T. C. Green, "Modeling, analysis and testing of autonomous operation of an inverter-based microgrid," *IEEE Trans. Power Electron.*, vol. 22, no. 2, pp. 613–625, Mar. 2007, doi: 10.1109/TPEL.2006.890003.

[5] D. E. Olivares, A. Mehrizi-Sani, A. H. Etemadi, C. A. Canizares, R. Iravani, M. Kazerani, A. H. Hajimiragha, O. Gomis-Bellmunt, M. Saeedifard, R. Palma-Behnke, G. A. Jimenez-Estevez, and N. D. Hatziargyriou, "Trends in microgrid control," *IEEE Trans. Smart Grid*, vol. 5, no. 4, pp. 1905–1919, Jul. 2014, doi: 10.1109/TSG.2013.2295514.

[6] M. Farrokhabadi et al., "Microgrid stability definitions, analysis, and examples," *IEEE Trans. Power Syst.*, vol. 35, no. 1, pp. 13–29, Jan. 2020, doi: 10.1109/TPWRS.2019.2925703.

[7] D. Pan, X. Wang, F. Liu, and R. Shi, "Transient stability of voltage-source converters with grid-forming control: A design-oriented study," *IEEE J. Emerg. Sel. Topics Power Electron.*, vol. 8, no. 2, pp. 1019–1033, Jun. 2020, doi: 10.1109/JESTPE.2019.2946310.

[8] H.-P. Beck and R. Hesse, "Virtual synchronous machine," in *Proc. 9th Int. Conf. Electr. Power Quality Utilisation*, Oct. 2007, pp. 1–6, doi: 10.1109/EPQU.2007.4424220.

[9] S. D'Arco and J. A. Suul, "Equivalence of virtual synchronous machines and frequency-droops for converter-based MicroGrids," *IEEE Trans. Smart Grid*, vol. 5, no. 1, pp. 394–395, Jan. 2014.

[10] J. Liu, Y. Miura, and T. Ise, "Comparison of dynamic characteristics between virtual synchronous generator and droop control in inverter-based distributed generators," *IEEE Trans. Power Electron.*, vol. 31, no. 5, pp. 3600–3611, May 2016.

[11] J. Fang, H. Li, Y. Tang, and F. Blaabjerg, "Distributed power system virtual inertia implemented by grid-connected power converters," *IEEE Trans. Power Electron.*, vol. 33, no. 10, pp. 8488–8499, Oct. 2018.

[12] M. H. Cintuglu, T. Youssef, and O. A. Mohammed, "Development and application of a real-time testbed for multiagent system interoperability: A case study on hierarchical microgrid control," *IEEE Trans. Smart Grid*, vol. 9, no. 3, pp. 1759–1768, May 2018.

[13] J. Driesen and K. Visscher, "Virtual synchronous generators," in *Proc. IEEE Power Energy Soc. Gen. Meeting*, Pittsburgh, PA, USA, Jul. 2008, pp. 1–6.

[14] E. Espina, J. Llanos, C. Burgos-Mellado, R. Cárdenas-Dobson, M. Martínez-Gómez, and D. Sáez, "Distributed control strategies for microgrids: An overview," *IEEE Access*, vol. 8, pp. 193412–193448, 2020, doi: 10.1109/ACCESS.2020.3032378.

[15] Energy Web. *What we do. Solutions: Data Exchange*. Accessed: Dec. 3, 2022. [Online]. Available: https://www.energyweb.org/solutions-data-exchange/

[16] C. Burgos-Mellado, C. Hernández-Carimán, R. Cárdenas, D. Sáez, M. Sumner, A. Costabeber, and H. K. M. Paredes, "Experimental evaluation of a CPT-based four-leg active power compensator for distributed generation," *IEEE J. Emerg. Sel. Topics Power Electron.*, vol. 5, no. 2, pp. 747–759, Jun. 2017.

[17] F. Guo, C. Wen, and Y.-D. D. Song, *Distributed Control and Optimization Technologies in Smart Grid Systems*. Boca Raton, FL, USA: CRC Press, 2017.

[18] J. Zhou, S. Kim, H. Zhang, Q. Sun, and R. Han, "Consensus-based distributed control for accurate reactive, harmonic, and imbalance power sharing in microgrids," *IEEE Trans. Smart Grid*, vol. 9, no. 4, pp. 2453–2467, Jul. 2018, doi: 10.1109/TSG.2016.2613143.

[19] C. Burgos-Mellado, J. J. Llanos, R. Cárdenas, D. Sáez, D. E. Olivares, M. Sumner, and A. Costabeber, "Distributed control strategy based on a consensus algorithm and on the conservative power theory for imbalance and harmonic sharing in 4-wire microgrids," *IEEE Trans. Smart Grid*, vol. 11, no. 2, pp. 1604–1619, Mar. 2020.

[20] F. L. Lewis, H. Zhang, K. Hengster-Movric, and A. Das, *Cooperative Control of Multi-Agent Systems* (Communications and Control Engineering). London, U.K.: Springer, 2014.

[21] J. Fu, G. Wen, W. Yu, T. Huang, and X. Yu, "Consensus of second-order multiagent systems with both velocity and input constraints," *IEEE Trans. Ind. Electron.*, vol. 66, no. 10, pp. 7946–7955, Oct. 2019, doi: 10.1109/TIE.2018.2879292.

[22] J. Qin, W. X. Zheng, and H. Gao, "Coordination of multiple agents with double-integrator dynamics under generalized interaction topologies," *IEEE Trans. Syst. Man, Cybern. B, Cybern.*, vol. 42, no. 1, pp. 44–57, Feb. 2012.

[23] V. Nasirian, Q. Shafiee, J. M. Guerrero, F. L. Lewis, and A. Davoudi, "Droop-free team-oriented control for AC distribution systems," in *Proc. IEEE Appl. Power Electron. Conf. Expo. (APEC)*, Mar. 2015, pp. 2911–2918, doi: 10.1109/APEC.2015.7104764.

[24] V. Nasirian, Q. Shafiee, J. M. Guerrero, F. L. Lewis, and A. Davoudi, "Droop-free distributed control for AC microgrids," *IEEE Trans. Power Electron.*, vol. 31, no. 2, pp. 1600–1617, Feb. 2016, doi: 10.1109/TPEL.2015.2414457.

[25] C. X. Rosero, M. Velasco, P. Martí, A. Camacho, J. Miret, and M. Castilla, "Active power sharing and frequency regulation in droop-free control for islanded microgrids under electrical and communication failures," *IEEE Trans. Ind. Electron.*, vol. 67, no. 8, pp. 6461–6472, Aug. 2020, doi: 10.1109/TIE.2019.2939959.

[26] M. A. Mahmud, M. J. Hossain, H. R. Pota, and A. M. T. Oo, "Robust nonlinear distributed controller design for active and reactive power sharing in islanded microgrids," *IEEE Trans. Energy Convers.*, vol. 29, no. 4, pp. 893–903, Dec. 2014, doi: 10.1109/tec.2014.2362763.
[27] J. M. Rey, P. P. Vergara, M. Castilla, A. Camacho, M. Velasco, and P. Martí, "Droop-free hierarchical control strategy for inverter-based AC microgrids," *IET Power Electron.*, vol. 13, no. 7, pp. 1403–1415, 2020, doi: 10.1049/iet-pel.2019.0705.
[28] Z. Wang, W. Wu, and B. Zhang, "A distributed quasi-Newton method for droop-free primary frequency control in autonomous microgrids," *IEEE Trans. Smart Grid*, vol. 9, no. 3, pp. 2214–2223, May 2018, doi: 10.1109/TSG.2016.2609422.
[29] Z. Zhang, C. Dou, D. Yue, and B. Zhang, "Predictive voltage hierarchical controller design for islanded microgrids under limited communication," *IEEE Trans. Circuits Syst. I, Reg. Papers*, vol. 69, no. 2, pp. 933–945, Feb. 2022, doi: 10.1109/TCSI.2021.3117048.
[30] J. Chen, D. Yue, C. Dou, Y. Li, G. P. Hancke, S. Weng, J. M. Guerrero, and X. Ding, "Distributed control of multi-functional grid-tied inverters for power quality improvement," *IEEE Trans. Circuits Syst. I, Reg. Papers*, vol. 68, no. 2, pp. 918–928, Feb. 2021, doi: 10.1109/TCSI.2020.3040253.
[31] J. Lai, X. Lu, A. Monti, and G. Liu, "Stochastic distributed pinning control for co-multi-inverter networks with a virtual leader," *IEEE Trans. Circuits Syst. II, Exp. Briefs*, vol. 67, no. 10, pp. 2094–2098, Oct. 2020, doi: 10.1109/TCSII.2019.2950764.
[32] C. Deng, Y. Wang, C. Wen, Y. Xu, and P. Lin, "Distributed resilient control for energy storage systems in cyber–physical microgrids," *IEEE Trans. Ind. Informat.*, vol. 17, no. 2, pp. 1331–1341, Feb. 2021, doi: 10.1109/TII.2020.2981549.
[33] C. Deng, Y. Wang, C. Wen, Y. Xu, and P. Lin, "Distributed resilient control for energy storage systems in cyber–physical microgrids," *IEEE Trans. Ind. Informat.*, vol. 17, no. 2, pp. 1331–1341, Feb. 2021, doi: 10.1109/TII.2020.2981549.
[34] I. Sowa and A. Monti, "On dynamics of communication-based distributed consensus control in islanded microgrids," in *Proc. Int. Conf. Smart Energy Syst. Technol. (SEST)*, 2022, pp. 1–6.
[35] R. Olfati-Saber, J. A. Fax, and R. M. Murray, "Consensus and cooperation in networked multi-agent systems," *Proc. IEEE*, vol. 95, no. 1, pp. 215–233, Jan. 2007, doi: 10.1109/JPROC.2006.887293.
[36] X. Wu, C. Shen, and R. Iravani, "A distributed, cooperative frequency and voltage control for microgrids," *IEEE Trans. Smart Grid*, vol. 9, no. 4, pp. 2764–2776, Jul. 2018, doi: 10.1109/TSG.2016.2619486.
[37] D. Breda, S. Maset, and R. Vermiglio, "Pseudospectral differencing methods for characteristic roots of delay differential equations," *SIAM J. Sci. Comput.*, vol. 27, no. 2, pp. 482–495, Jan. 2005, doi: 10.1137/030601600
[38] D. Breda, S. Maset, and R. Vermiglio, "Pseudospectral approximation of eigenvalues of derivative operators with non-local boundary conditions," *Appl. Numer. Math.*, vol. 56, nos. 3–4, pp. 318–331, Mar. 2006, doi: 10.1016/j.apnum.2005.04.011.
[39] F. Milan and M. Anghel, "Impact of time delays on power system stability," *IEEE Trans. Circuits Syst. I, Reg. Papers*, vol. 59, no. 4, pp. 889–900, Apr. 2012, doi: 10.1109/TCSI.2011.2169744.
[40] D. Das, "Reconfiguration of distribution system using fuzzy multi-objective approach," *Int. J. Electr. Power Energy Syst.*, vol. 28, no. 5, pp. 331–338, Jun. 2006.

IGOR SOWA received the dual M.Sc. degree in electrical engineering from KTH University, Stockholm, Sweden, and UPC University, Barcelona, Spain, in 2016. He is currently pursuing the Ph.D. degree with RWTH University, Aachen, Germany. He is also a Research Associate with the Institute for Complex Power Systems, RWTH University. His research interests include power system dynamics and control, and communication, automation, and monitoring in modern power systems and microgrids.

ANTONELLO MONTI (Senior Member, IEEE) received the M.Sc. (summa cum laude) and Ph.D. degrees in electrical engineering from Politecnico di Milano, Italy, in 1989 and 1994, respectively. He started his career with Ansaldo Industria and then moved to Politecnico di Milano as an Assistant Professor, in 1995. In 2000, he joined the Department of Electrical Engineering, University of South Carolina, USA, as an Associate Professor, and then a Full Professor. Since 2008, he has been the Director of the E. ON Energy Research Center, Institute for Automation of Complex Power System, RWTH Aachen University. He is the author or coauthor of more than 300 peer-reviewed papers published in international journals and proceedings of international conferences. He was a recipient of the 2017 IEEE Innovation in Societal Infrastructure Award. He is a member of the editorial board of the *SEGAN* (Elsevier) and a member of the founding board of the *Energy Informatics* (Springer). He is an Associate Editor of the IEEE System Journal and *IEEE Electrification Magazine*.